$\pi^* \rightarrow n$ Fluorescence Transition in Formaldehyde in Aqueous Solution: A Combined Quantum Chemical Statistical Mechanical Study

Anders Öhrn* and Gunnar Karlström

Department of Theoretical Chemistry, Chemical Center, P.O.B. 124, S-221 00 Lund, Sweden

Received: October 5, 2005; In Final Form: December 20, 2005

The solvent shift to the fluorescence transition $\pi^* \rightarrow n$ in formaldehyde in aqueous solution is theoretically analyzed. The solvent model has explicit representation of the solvent and uses the complete active space state interaction (CASSI) method to obtain a description of the wave function of the solute similar to what the complete active space self-consistent-field (CASSCF) method would give. In the description of the solute−solvent interaction the discrete set of solvent molecules perturb the solute not only through an electrostatic perturbation but also through a nonelectrostatic operator. The latter describes in a way analogous to pseudopotential theory the effect the Pauli principle has on the solute embedded in the solvent. This way the exchange repulsion between solute and solvent is accounted for which therefore can be anisotropic. The best estimate of the average shift is a blue shift of 0.003 eV, and for the current transition the nonelectrostatic perturbation broadens the distribution but has no significant effect on the average shift.

1. Introduction

Quantum chemistry has, for understandable reasons, evolved through studies of isolated molecules and is now in a state where high accuracy can be attained in, for example, theoretical studies of the spectroscopy of such systems. Many important parts of chemistry, on the other hand, take place in large molecular aggregates that conceptually often are separated in interacting fragments: the distinction between solute and solvent is the most prominent, if not the only, such separation. To be able to treat these aggregates in quantum and computational chemistry, this separation has been adopted and effective environment models has been formulated with the continuum solvent models being the most conspicuous exemplification.[1−3] With increasing performance of computer processors, though, more detailed models are now feasible, and studies with explicit solvent models are becoming more common.

In biochemistry—the primary example of chemistry in large aggregates—fluorescence spectroscopy, i.e. the radiation emitted when a system passes from an electronically excited singlet state to a lower state, and its solvent effect, has become a useful analytical technique.[4−7] Structural change in proteins is one thing that in some cases can be monitored through the fluorescence spectrum and its shift when the environment of the fluorescent fragment—tryptophan to name one—is modified upon structural change.

In the present study we investigate the solvent shift to the $\pi^* \rightarrow n$ fluorescence transition in formaldehyde in aqueous solution with a recently developed quantum chemical solvent model with explicit solvent representation.[8] Admittedly, formaldehyde is not an example of a molecule of biochemical interest in the respect discussed above—in fact, formaldehyde does not even exist in aqueous solution since it to a large degree reacts with water and forms methylenediol. Still, being the simplest molecule with a carbonyl functional group, this solute−solvent system has been the subject of several theoretical studies and has become something of a steppingstone for solvent models that at a later stage could be applied to systems interesting in the above sense. Our results are compared to previous studies.[9−13]

2. Method

Since the details of the model, called QMSTAT, are available elsewhere, the presentation of the method will be limited to the most salient features.[8]

QMSTAT is an effective discrete solvent model. In other words, the modeled system is divided into a central part, treated with a quantum chemical method (vide infra), and a complement that acts as a perturbation to the central part; the discreteness signifies that the complement is represented as a set of individual solvent molecules. However, macroscopic solutions are complex systems with long-ranged interactions; hence, an explicit treatment of all relevant solvent degrees of freedom is infeasible, and a truncation scheme is necessary. Our choice is to spherically encompass the quantum chemical part and a finite set of solvent molecules with a dielectric continuum; the continuum reaction field is calculated within the image-charge approximation.[14] The effective treatment of the quantum chemical region makes it suitable to place it at or close to the center of the spherical cavity, and since the number of explicit solvent molecules is of the order 100, there is no obvious advantage to make the boundary nonspherical (this is preferable, however, if fewer explicit solvent molecules are included[15,16]). Boltzmann-distributed properties are obtained with the Metropolis−Monte Carlo algorithm;[17] practical details of the cavity simulation are available elsewhere.[8,18]

The solvent, which in the present study is water, is described with an early version of the NEMO force field.[19] The charge density is expanded in four point charges of such magnitude and location that the dipole and quadrupole moments of water are reproduced. The force field is polarizable and includes three point polarizabilities per molecule for that purpose.

Every solvent model with an explicit representation of the solvent has to select some solute−solvent configurations for the thermal averaging; the approach adopted by most researchers

10.1021/jp055678l CCC: $33.50
Published on Web 01/18/2006

is to collect these configurations from an all-classical simulation of the system under study. Consequently, the configurations used to compute the statistical distribution of any property obtained with the quantum chemical model will not converge toward the exact Boltzmann distribution since the configurations are distributed according to the all-classical potential—a potential which necessarily differs from the combined quantum chemical statistical mechanical potential in some respects. Obviously, with a good classical force field—"good" meaning able to reproduce the quantum-classical solute−solvent interaction—this error can be made small and insignificant compared to other limitations of the various models. Further, the usual approach also makes the model dependent on parameters to the all-classical simulation, a fact that for ground state simulations is only mildly restrictive given the vast number of classical molecular simulations and force fields available in the literature; for excited states in equilibrium with the solvent far fewer parameters and applicable models are available so this dependence becomes more restrictive. To circumvent these problems, we use *the same potential for both simulation and quantum chemical calculations* in QMSTAT; i.e., in every Monte Carlo step a quantum chemical problem has to be solved to obtain the effective solute wave function.

Considering that we aim at a description of excited states, the complete active space self-consistent-field (CASSCF) method would be suitable to describe the solute wave function since this method has proven itself well-suited for handling such states.[20−24] Because of the need to solve a quantum chemical problem in each Monte Carlo step, the CASSCF method cannot be used directly, however, since it would make QMSTAT too computationally expensive. (A major portion of the computer time in CASSCF is allocated to two-electron integral transformations.) To retain several of the advantageous features of the CASSCF method and still be able to solve a quantum chemical problem in each Monte Carlo step, we use a construction based on the complete active space state interaction (CASSI) method.[25,26] Given a set of CASSCF wave functions as input, the CASSI method computes a set of orthogonal noninteracting eigenstates to the Hamiltonian at hand that span the same subspace as the CASSCF wave functions (which can be slightly nonorthogonal due to that both CI coefficients and molecular orbitals are varied); typical application of CASSI is to compute matrix elements between different states, such as transition dipole moments and more recently spin−orbit couplings.[27] In QMSTAT the wave function for the solvated molecule, Ψ^Q, is written as a linear combination of a set of CASSI states, $\{\Psi_j\}_{j=1,...,N}$:

$$\Psi_i^Q = \sum_j^N c_{ij}\Psi_j \tag{1}$$

Then given the effective Hamiltonian for the solute, $H_{\text{eff}} = H_0 + V_{\text{solv}}$, the variational method is used to approximately solve the Schrödinger equation; since the ansatz is linear and the CASSI state functions are mutually orthogonal, the solution is readily obtained upon diagonalization of the matrix $\{\langle\Psi_i|H_0 + V_{\text{solv}}|\Psi_j\rangle\}_{i,j=1,...,N}$. Observe that in no stage of the solution of the quantum chemical problem in QMSTAT there is a need to store or transform two-electron integrals. With a suitable set of CASSCF wave functions as input to CASSI (how they are prepared for this particular study is presented in a later section) we believe that this ansatz adequately emulates the CASSCF wave function had it been used. The perturbation from the solvent V_{solv} is not allowed to be too large for this to be true since then the projection of the correct CASSCF wave function onto the subspace spanned by the CASSI state functions will be too dissimilar from the correct wave function. On the other hand, for a large perturbation any effective treatment of the solute−solvent system will falter and at least some solvent molecules have to be included into the quantum chemical region such as in the Car−Parinello method or in the method by Loeffler and Rode.[28]

To proceed, the solvent perturbation V_{solv} has to be formulated. Above the usual electrostatic perturbation, QMSTAT also includes a nonelectrostatic perturbation V_{nel} which models how the solvent density through the Pauli principle influences the solute wave function; in the present article we only recapitulate the features of and arguments for this contribution to the total perturbation.

Spectroscopic studies of benzene in cryogenic fluids such as argon and helium led Nowak and Bernstein to conclude that repulsive interactions had an important effect on the spectrum in solvated benzene.[29] Also, Zipp and Kauzmann discuss the possibility that the repulsive interaction between solute and solvent has to be accounted for to explain the pressure effects they find on a number of absorption spectra in solution.[30] In a theoretical discussion of solvent shifts, Bayliss and McRae introduce the notion of *packing strain* to describe the unfavorable packing of the vertically excited state of the solute in the surrounding solvent.[31] Price et al. also mention that steric interactions between the excited state and its surrounding can have an effect on the perichromism (a general term for the shift caused by any type of surrounding, see ref 32) of molecules.[33] In addition to this, problems with the repulsive interaction between solute and solvent have been pointed out in discussions of QM/MM models, for example, the risk of variational distortion caused by solute density being too attracted to the point charges in the solvent;[34,35] in other words, Pauli-forbidden intruder states enter through the solvent perturbation, which may cause highly nonphysical states to be occupied.[36] Stratt and coworkers have in a number of articles made theoretical studies of the solvent shift of model systems using simple hard-sphere liquids as solvents, later augmented with Drude oscillators to describe polarization.[37−39] Their conclusions are that the pure steric interaction between solute and solvent engenders a blue shift to the absorption band as well as a broader statistical distribution of the same. Interestingly, they also find that an important feature of the hard-sphere solvation is the collective shape of the particles closest to the solute and the variations of the geometry of the solvation shell; this coupled anisotropy in repulsion, polarization, and solvation shell shape was also found in a work in our laboratory on the solvation of four monatomic ions in their ground state with a version of the QMSTAT model with a Hartree−Fock wave function.[40]

Conclusively, there are several arguments in favor of including a perturbation of steric origin on the solute from the solvent. QMSTAT has from the beginning included such a perturbation, which in ref 8 was reformulated somewhat compared to earlier versions of the model.[18,40−43] The nonelectrostatic perturbation operator reads

$$V_{\text{nel}} = d\sum_{k\in\Omega}\sum_{n=1}^{N}\epsilon_n|\phi_{n,k}^S\rangle\langle\phi_{n,k}^S| \tag{2}$$

where $|\phi_{n,k}^S\rangle$ is the nth occupied molecular orbital (MO) on the kth solvent molecule in the set Ω; ϵ_n is the nth orbital energy, and d is a parameter that needs to be fitted to a reference (vide infra); in a given configuration the solvent molecules closer to any atom of the solute than some user-defined cutoff radius are

included in the set Ω. To argue for the form of V_{nel}, we refer to pseudopotential theory and symmetry-adapted perturbation theory.

The former theory was originally derived to treat the steric interaction of the valence electrons with the core electrons in atoms not with Lagrangian multipliers as in the Hartree−Fock equations, but rather with a so-called pseudopotential that modifies the Hamiltonian for the valence electrons.[44] The applications of pseudopotential theory has extended beyond this and now also includes, for example, the connection of intramolecular fractions to one another as well as effectively treating the crystalline environment in solid-state physics.[45,46] (See especially the work by Barandiarán and Seijo in ref 45, which has a nonlocal exchange potential similar to ours.) Applications of pseudopotentials to solvent models have, apart from the previous QMSTAT calculations, been used in various contexts and formulations.[47−50] In the work by Schnitker and Rossky on the solvated electron a pseudopotential for the electron−water interaction is absolutely vital; otherwise, the electron would not be bound and therefore not display any discrete absorption spectrum, which Hart and Boag were the first to confirm that it indeed does.[50,51]

With the latter theory it has been shown that the short-range repulsion between molecules to first order is proportional to the wave function overlap, *S*, between the interacting partners raised to the power of two.[52−54] The expression for V_{nel} is consonant with this result, since the matrix element $\langle\Psi_i| V_{nel}|\Psi_j\rangle$ becomes a sum of products of two overlaps between the solute and the solvent molecules in Ω. The symmetry-adapted perturbation expansion does however include higher order terms as well. In QMSTAT such terms are added, although not to V_{nel} but rather to the total energy. Added there, they have no *direct* influence on the variation of the solute wave function. Most of the repulsion, though, especially at equilibrium and longer distances, comes from the term of order S^2 in V_{nel}.

As a final remark we point out that, unlike in our previous work with this model, the electric field is not damped at short range to compensate for the charge overlap; no convergence problems in solving the polarization equations were encountered, and the V_{nel} will in part model the charge overlap.

3. Calculation Protocol

The atomic natural orbital (ANO) basis set is used in all our quantum chemical calculations.[55,56] Two different contractions are used: a more contracted basis set called Ano.s(I) throughout the text (C,O 5s4p1d contraction, H 3s2p contraction) and a less contracted called Ano.s(II) (C,O 7s6p3d contraction, H 4s3p contraction).

All CASSCF calculations are performed with four active electrons and the π, n, and π^* orbitals in the active space. To prepare an input set of state functions to CASSI, we do as follows: state-average CASSCF (SA-CASSCF) calculations with equal weight to ground and first excited state (the $S_1(n,\pi^*)$ state) are performed with a homogeneous electric field of strength 0.003 au directed in sequence along all three axes in both directions as well as one calculation without any field. Fourteen states, some of which are overlapping significantly, follow from these in total seven calculations. CASSI, given these states, produces 14 eigenstates to the unperturbed Hamiltonian where the two lowest will be good estimates of the ground and first excited state, while the remaining 12 will be needed in the description of the polarization of the former.

Since a fluorescence spectrum is to be computed, the structure of the excited state needs to be relaxed. An excited-state geometry optimization is performed with analytical gradients (which due to the nonvariational nature of the SA-CASSCF wave function are nontrivial to compute).[57] The second root to the CASSI construction described above is close but not exactly equal to the second root to the SA-CASSCF equations since some further correlation is introduced through the CASSI procedure; thus, we expect small modifications of the optimal geometry going from CASSCF to CASSI—modifications established by a zero-order method, i.e., energies of nearby structures are compared.

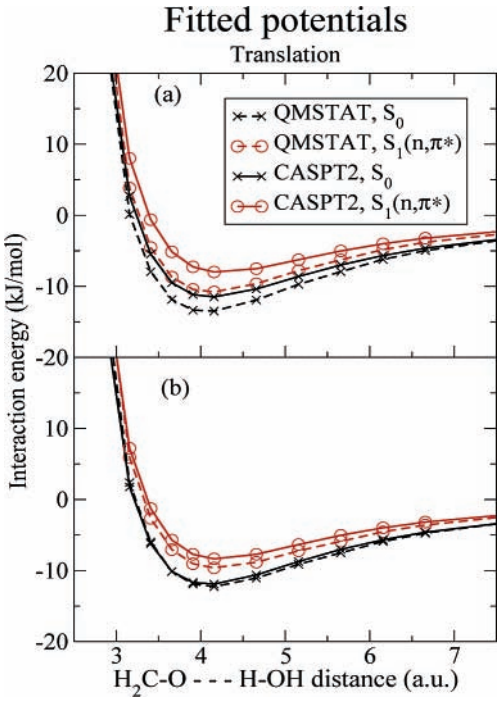

Figure 1. CASPT2 counterpoise corrected supermolecular potential (translation) for the ground and the $S_1(n,\pi^*)$ state of formaldehyde in the optimal geometry for the excited state; also, the QMSTAT fit. Referring to Figure 3, $\alpha = 180°$; $\gamma = 180°$. (a) Ano.s(I) basis set, (b) Ano.s(II) basis set.

With the CASSI-optimal structure for the first excited state given, a supermolecular reference potential is needed to fit the parameters in QMSTAT to. Since dispersion is included in the QMSTAT solute−solvent interaction, dynamic correlation is required. A suitable reference is thus the complete active space with second-order perturbation correction (CASPT2) potential—a method known to perform well for quantitative calculations on excited states.[58−60] All supermolecular potentials are counterpoise corrected, an accurate and sound correction to the basis set superposition error.[61,62]

All quantum chemical calculations are performed with the MOLCAS program package.[63]

After initial equilibration, a total of 7 million Monte Carlo steps are performed in each simulation. Every hundredth configuration is stored for subsequent analysis; in other words, 70 000 configurations are used to compute all thermal averages.

4. Results

4.1. The Pair Potential. The fitted QMSTAT potentials for the singlet ground state, S_0, and the first singlet excited state, $S_1(n,\pi^*)$, are shown in Figure 1 for a translational degree of freedom and in Figure 2 for a rotational degree of freedom as explained in the captions and in Figure 3. Parameters are listed in Table 1.

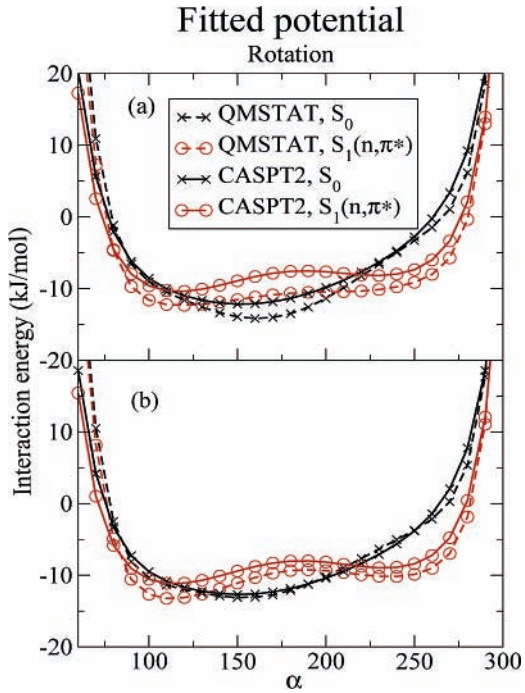

Figure 2. CASPT2 counterpoise corrected supermolecular potential (rotation) for the ground and the $S_1(n,\pi^*)$ state of formaldehyde in the optimal geometry for the excited state; also, the QMSTAT fit. Referring to Figure 3, $r = 4.1$ au; $\gamma = 180°$. (a) Ano.s(I) basis set, (b) Ano.s(II) basis set.

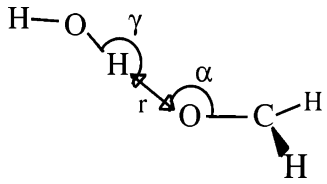

Figure 3. Definition of geometrical parameters to the QMSTAT and CASPT2 potentials.

TABLE 1: Parameters for the Excited Formaldehyde−Water System[a]

interaction	parameter	Ano.s(I)	Ano.s(II)
repulsion	d	−0.48	−0.46
	β_6	0.3	0.3
	Ω cutoff (au)	7.0	7.0
dispersion	$D_{C,O}$	75.0	75.0
	$D_{C,H}$	9.0	9.0
	$D_{O,O}$	37.0	37.0
	$D_{O,H}$	4.5	4.5
	$D_{H,O}$	13.0	13.0
	$D_{H,H}$	1.7	1.7

[a] All relevant equations are available in a previous publication;[8] the solvent−solvent parameters are given in ref 19.

For both the translational and the rotational potential surface intersection and for both basis sets, there is satisfactory agreement between the simplified QMSTAT potential and the counterpoise-corrected CASPT2 supermolecular potential. With the CASSI construction for the solute in QMSTAT the density is almost equivalent to the CASSCF density. Thus, the density correction which the perturbation treatment brings about is not included; such treatment typically leads to slight modifications of the electric moments of the molecule. This is the probable reason for the almost constant vertical displacement of the QMSTAT potential relative the CASPT2 potential in Figure 2 and the somewhat too attractive force manifest in Figure 1; judging by the small difference the modification is, as anticipated, minor. Further, since only energy differences matter in the simulation and the subsequent analysis, this discrepancy between the potentials is of little importance. We also observe that both states are described well with only one value on the parameter d in V_{nel}.

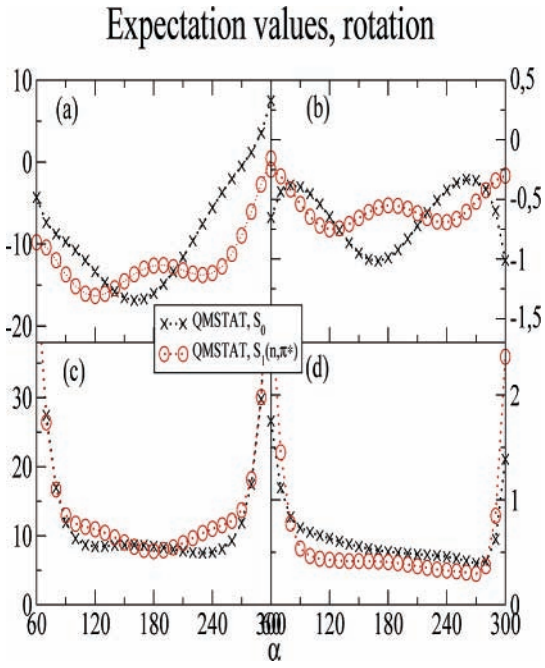

Figure 4. For the relaxed wave function in QMSTAT with the Ano.s(I) basis set, (a) is $\langle V_{el} \rangle + E_{elnuc}$ where E_{elnuc} is the interaction between solvent point charges and nuclei in formaldehyde, (b) is $\langle V_{pol} \rangle + E_{polnuc}$ where E_{polnuc} is the interaction between solvent induced dipoles and nuclei in formaldehyde, (c) is $\langle V_{nel} \rangle$, and (d) is $\langle H_0 \rangle$; observe the different energy scales (in kJ/mol).

From the CASPT2 potentials—interesting in themselves—we conclude: (1) There is a significant decrease in strength of the hydrogen bond between formaldehyde and water when going from the ground state to the excited state (or vice versa). The same mechanism is usually cited as the reason for the blue solvent shift to the $n \rightarrow \pi^*$ transitions in aldehydes and ketones in protic solvents. The weakening is explained—speaking in terms of orbitals—as brought about by the removal of electron density from the nonbonding n-orbital of the oxygen atom; hence, less negative charge is left to favorably interact with the partially positive hydrogen atom of the nearby water molecule. (2) But also, going from the one state to the other does not simply lead to a rescaling of the interaction as the variation in the rotational degree of freedom (Figure 2) reveals: the cusp at 180° in the $S_1(n,\pi^*)$ intermolecular potential is a feature not present in the potential for the ground state. With the total energy decomposed in separate terms in QMSTAT, we are able to investigate the origin of this cusp. In Figure 4 the expectation values for the Ano.s(I) calculation of the four operators in the QMSTAT solute energy expression, H_0 (the intramolecular interaction), V_{el} (the interaction between solvent point charges and solute density), V_{pol} (the interaction between solvent induced dipoles and solute density), and V_{nel} (the nonelectrostatic interaction) along the rotational degree of freedom are shown. Both $\langle V_{el} \rangle$ and $\langle V_{pol} \rangle$ display the same cusp; hence, electrostatic interactions are the likely cause of the cusp. Further evidence comes from the observation that the molecular dipole and polarizability of the two states (listed in Table 2) will upon transition change not only in magnitude but also in direction and anisotropy, respectively. Upon comparison of parts a and c of Figure 4, we see that $\langle V_{nel} \rangle$ for the excited state actually

TABLE 2: Properties in Atomic Units of the Wave Function Used in QMSTAT (Eq 1) with the Two Basis Sets, for Dipole (μ_x,μ_y,μ_z) and for Polarizability ($\alpha_{xx},\alpha_{yy},\alpha_{yz},\alpha_{zz}$)

property	basis set	S_0	$S_1(n,\pi^*)$
vacuum energy	Ano.s(I)	−113.89606	−113.81565
	Ano.s(II)	−113.89797	−113.81796
dipole	Ano.s(I)	(0.0,−0.1968,−0.9219)	(0.0,−0.2222,−0.5720)
	Ano.s(II)	(0.0,−0.1970,−0.9127)	(0.0,−0.2309,−0.5574)
polarizability	Ano.s(I)	(14.4,12.2,0.22,20.5)	(14.2,12.9,0.30,16.4)
	Ano.s(II)	(15.6,13.7,0.21,21.1)	(15.7,14.6,0.23,17.8)

TABLE 3: Optimized Geometry for the $S_1(n,\pi^*)$ State with SA-CASSCF and CASSI for the Two Types of Basis Set[a]

method	basis set	C−O	C−H	H−C−H	wiggle
SA-CASSCF	Ano.s(I)	2.56	2.03	118.6	39.7
	Ano.s(II)	2.56	2.03	118.5	39.6
CASSI	Ano.s(I)	2.57	2.03[b]	118.8	39.1
	Ano.s(II)	2.57	2.03[b]	118.4	39.6

[a]Bond lengths in atomic units; the angle (in deg) between the vector along the C−O bond and the plane definied by the hydrogen atoms and the carbon atom is the wiggle angle; zero degrees means planar structure. [b] The C−H distance was not optimized in CASSI, but kept fixed at the value from the SA-CASSCF calculation.

features a small "inverted cusp" with more repulsion at angles where $\langle V_{el}\rangle$ and $\langle V_{pol}\rangle$ are most favorable; a possible explanation is that at favorable angles (around 110° and 240°) greater polarization of formaldehyde leads to greater intermolecular overlap and with that more repulsion through V_{nel}.

4.2. Solute and Solvent Structure. The $S_1(n,\pi^*)$ state of formaldehyde is known to be nonplanar; this was first conjectured by Walsh in 1953, with spectroscopic results supporting the conjecture a few years later.[64,65] Highly correlated multireference configuration interaction (MRCI) and CASPT2 calculations reach the same conclusion and several other quantum chemical methods as well (see table 2 in ref 68).[66−68] Laane discusses the nonplanarity of the $S_k(n,\pi^*)$ state of other ketones and aldehydes.[69] In Table 3 our optimized geometry for formaldehyde is reported. As seen, the difference between CASSCF and CASSI in this respect is very small.

If there are low-frequency nuclear degrees of freedom in the solute and a significant coupling between solute and solvent, there is a possibility that the solvent through its perturbation modifies the solute structure and consequently the spectrum. Since it would increase the computational effort substantially to make the solute structure flexible, we keep it fixed. Still, working within that restriction, the most suitable structure to use is the free energy optimal structure. From configurations sampled with the gas-phase structure we carry out free energy perturbation calculations to investigate whether the free energy can be lowered by small geometry modifications.[70,71] With neither basis set can the free energy be lowered with the available statistical precision and applied bond length and angle variation (0.01 au and 0.1°, respectively). Hence, the fixed formaldehyde geometry used in all calculations is the one reported in Table 3 for the corresponding basis set.

In Figure 5a,b the normalized radial distribution functions (the carbonyl oxygen atom in origo) are shown for the two basis sets. They give some information about the structure of the solvent, but as is apparent from the pair potentials angular dependence is expected to be relevant and this dependence is more difficult to visualize two-dimensionally. The distribution functions reflect what we know from the pair potentials, namely, that there is a weaker interaction between the carbonyl oxygen and the solvent than in the ground state where a pronounced peak occurs in the hydrogen distribution, see Figure 5c,d where

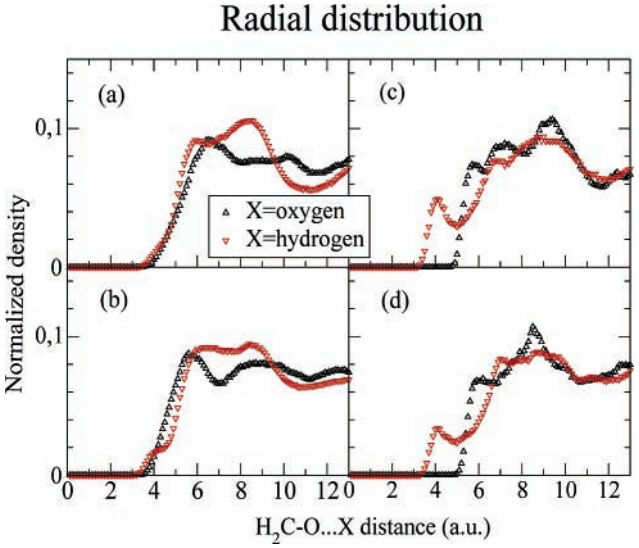

Figure 5. Normalized radial distribution functions with the oxygen atom in formaldehyde as origo with (a) the Ano.s(I) basis set and (b) the Ano.s(II) basis set for the excited state $S_1(n,\pi^*)$. Also the distributions for the ground state in equilibrium for (c) the Ano.s(I) and (d) Ano.s(II) basis set (data from ref 8).

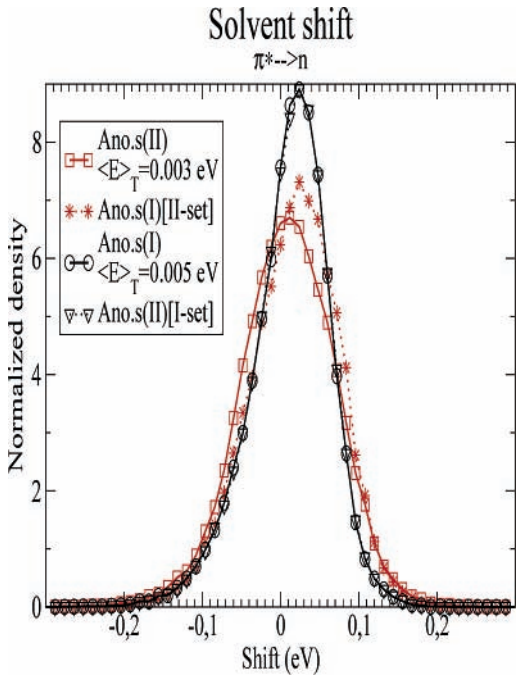

Figure 6. Solvent shift distributions for the $\pi^* \rightarrow n$ transition in aqueous solution computed with both basis sets. Also, the shifts obtained when configurations sampled for the one basis set is used to formulate V_{solv} but applied to the wave function in the other basis set; Ano.(I)[II-set], for example, means that the wave function is expanded in the Ano.s(I) basis set while the set of configurations are sampled from a simulation with the Ano.s(II) wave function.

data are taken from the work presented in ref 8. Also, in contrast to the ground state where the carbonyl oxygen is preferably solvated by the hydrogen atoms of the water molecules, the hydrogen atoms are on average only slightly closer to the carbonyl oxygen atom than the oxygen atom on the water molecules. Conclusively, only little radial structure is imposed on the solvent around the oxygen atom in the $S_1(n,\pi^*)$ state of formaldehyde.

4.3. Solvent Shift. In Figure 6 the normalized solvent shift distributions for the $\pi^* \rightarrow n$ transition are shown for the two

basis sets. A positive shift means that the transition is blue-shifted, in other words, that the energy difference between final and initial state is increased upon solvation which, as a consequence of the final state being lower in energy than the initial state, means that the former state is more stabilized by the solvation than the latter state. The average shift is almost 0 eV for both basis sets, and the small difference cannot be considered to be statistically significant. Both distributions have a minor asymmetry with respect to their maximum with a tail extending to negative shifts. A significant difference between the distributions of the two calculations is the width: the larger basis set gives rise to a wider distribution. To elucidate the source of this difference and simultaneously analyze the causes of the shifts, we make a joint configuration space-wave function space test as well as investigate the effect of V_{nel} and the polarization.

In Figure 6 there are two additional curves above the ones mentioned in the previous paragraph. The one named "Ano.s(I)[II-set]" is obtained as follows: the stored configurations from the simulation with the larger Ano.s(II) basis set are used to formulate the perturbation V_{solv}, but the quantum chemical problem is solved in the space expanded in the smaller Ano.s(I) basis set. Since the configurations no longer are distributed according to the correct Boltzmann distribution, they cannot be equally weighted—as is the case in the Metropolis—Monte Carlo algorithm—but have to be reweighted with the proper Boltzmann factor, with the effect that the quality of the statistics is worsened. The curve labeled "Ano.s(II)[I-set]" is obtained doing the opposite configuration/basis set interchange. First, the Ano.s(II)[I-set] curve is as good as equivalent to the Ano.s(I) curve. This relation indicates that, within the configuration space that belongs to the system with the Ano.s(I) wave function, the Ano.s(II) and Ano.s(I) wave functions have very similar properties, in other words, that the difference between the Hilbert subspaces that the two wave functions occupy is minute. Second, the Ano.s(I)[II-set] distribution differs more from the Ano.s(II) curve and also seems to approach the Ano.s(I) distribution. This relation indicates that, within the configuration subspace properly distributed to the Ano.s(II) system, the wave function expanded in the smaller Ano.s(I) basis set occupies—in comparison with the situation above—a more dissimilar wave function space than the wave function to which the configurations are distributed. That the Ano.s(I)-[II-set] curve fail to coincide with the Ano.s(I) curve is probably due to the diminution in quality of the statistics when the data is reweighted. Conclusively, the wave function expanded in the Ano.s(II) basis set have features, not manifested by the Ano.s-(I) wave function, that influences the Boltzmann distribution making at least some configurations significantly more probable than for the Ano.s(I) system.

To pursue the analysis further and establish what qualitative features in the solute−solvent interaction that differ between the differently expanded wave functions, we present in Figure 7 the correlation between the proper shifts shown in Figure 6 and shifts obtained with the nonelectrostatic perturbation absent. The latter shifts are acquired by computing the shifts with the repulsion parameters set to zero for the configurations stored from the simulations. In contrast to our study of the $n \rightarrow \pi^*$ absorption, V_{nel}, on average, contributes to neither a blue shift nor a red shift. But it does contribute to the width of the distribution. If V_{nel} for a particular configuration decreases the energy difference (in Figure 7 the corresponding point lies below the 1:1 line), the likely cause is that the different electronic structure of the ground state overlaps more with the solvent

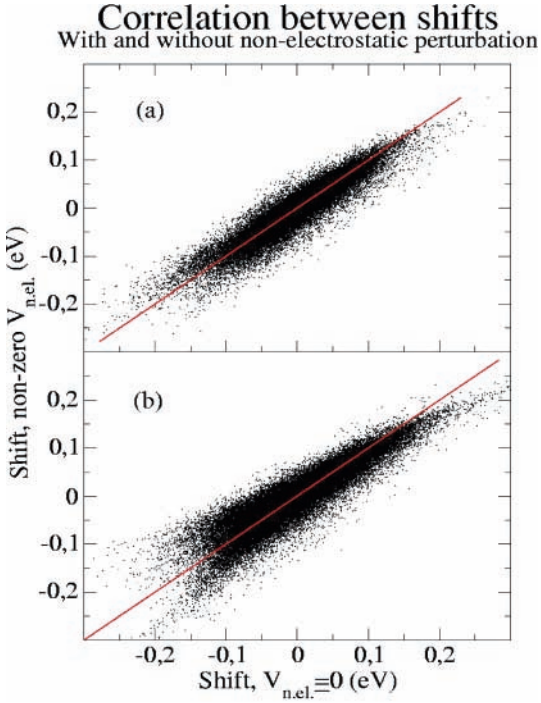

Figure 7. Correlation between shifts computed with and without the nonelectrostatic perturbation for (a) the Ano.s(I) basis set and (b) the Ano.s(II) basis set.

that has adapted to the structure of the excited state. To explain the opposite effect, we propose—like in ref 8—the following two plausible mechanisms: The easiest to apprehend is the opposite of the mechanism outlined above, namely, that upon fluorescence the shape of the ground state happens to better "fit" the solvation shell than did the initial excited state; since excited states usually are more diffuse than ground states, this mechanism is probably more important than upon absorption. The other mechanism derives from the coupling of the various perturbations: they are not independent. As was shown in our previous study in ref 8, the nonelectrostatic perturbation can modify the electronic structure so the electrostatic interaction of the final state becomes more like the initial state and consequently more favorable—a mechanism that in this case would lead to points above the 1:1 line.

The collective widths of the points in parts a and b of Figure 7 are comparable. Thus, differences in the nonelectrostatic interaction does not appear to be the cause of the broader distribution of the Ano.s(II) basis set in Figure 6. Through a perturbation calculation with a homogeneous electric field of strength 0.005 au applied on the formaldehyde in either of its two states, the molecular polarizabilities can be computed; they are included in Table 2. The molecular polarizability is larger in the larger basis as could be expected. Since the molecular polarizability only can give an estimate of the response to an inhomogeneous field from a microscopic surrounding, we also establish the distribution of induced dipoles (see Figure 8). For both states the average induced dipole as well as the standard deviation is larger for the larger basis set. This greater flexibility and variation of the charge distribution expanded in the larger basis set is the probable cause of the greater width of the Ano.s(II) curve in Figure 6: the interaction for initial and final state is more diverse in the larger basis set, and thus there will be more configurations with larger shifts in either direction depending on which state that is most stabilized.

If the environment is treated as a dielectric medium, the average solvent shift to the fluorescence peak is toward shorter

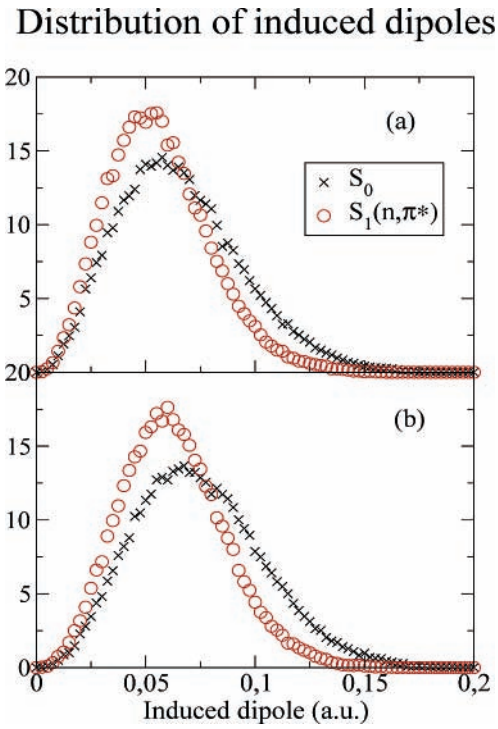

Figure 8. Distribution of induced dipole for (a) the Ano.s(I) and the (b) Ano.s(II) basis set. For (a) the averages are 0.0645 and 0.0549 au for state S_0 and $S_1(n,\pi^*)$, respectively; for (b) the averages are 0.0733 and 0.0615 au. The standard deviations are for (a) 0.0286 and 0.0233 au for the states S_0 and $S_1(n,\pi^*)$; for (b) 0.0294 and 0.0237 au.

wavelengths since the dipole in the final state is greater than in the initial state by almost a factor of 2 (see Table 2). Since the nonelectrostatic perturbation contributes with at most a minor shift in either direction, packing strain cannot be invoked to explain the lack of observed shift. Specific interactions between solute and solvent is then the likeliest cause of this observation. Although the ground state can interact most favorably with the solvent—especially forming strong hydrogen bonds, see Figure 1—every thermal average is computed with a distribution function as weight, and as is evident from Figures 2 and 5, the equilibrium configurations of the excited state are differently distributed from what would have been the free energy optimal distribution for the ground state. As the major reason for our observed lack of significant blue shift, we therefore propose to be that the specific interactions are optimized for the excited states and because of this fail to realize their full strength in the vertically deexcited state.

For reasons described above no experimental data are available to compare with. For hydrated acetone, with a similar excitation process as formaldehyde, experimental data are available;[73,74] see also Table 1 in ref 75. There a blue shift of at least 0.2 eV is found in several different solvents with different permittivities and hydrogen bond formation properties. This is noteworthy since if a strong electrostatic interaction between solute and solvent is present, it can undergo a significant change upon transition, while if the permittivity of the medium is low, the solute−solvent interation is weaker and the shift is expected to be smaller. A separate study of hydrated acetone is in progress, and before it is completed it is difficult to connect the acetone experiments and the present theoretical results on formaldehyde. To obtain a blue shift either the excited state of the solute has to be less stabilized by the solvent or the ground state more stabilized, or a combination of both; it is possible to imagine physical reasons for this to happen when going from formaldehyde to acetone. Then, of course, deficiencies of the model are possible, but their direction and magnitude remain to be established.

TABLE 4: Compilation of Results for Solvent Shift to the $\pi^* \rightarrow n$ Transition in Formaldehyde in Aqueous Solution[a]

solvent model	QM method	shift (eV)	ref
all classical molecular dynamics simulation	none	≈0.22	9
integral equation theory	HF	0.035	11
nonequilibrium continuum model	CIS	0.082	12
nonequilibrium continuum model	CISD	0.033	12
clusters from Monte Carlo simulation	INDO/CIS	0.20	13
QM/MM Monte Carlo simulation	CASSI	0.003	present

[a] The values are for the nonplanar C_s structure of formaldehyde.

4.4. Comparison with Other Studies. In Table 4 the average solvent shifts obtained by other researchers are summarized together with our best estimate. Levy et al. have from classical molecular dynamics calculations with interactions parameters and partial charges (no polarizabilities) to the excited formaldehyde derived from Hartree−Fock (HF) calculations, obtained a shift to the fluorescence of ∼0.22 eV.[9] In an all classical simulation there will, of course, be features left out of the solute−solvent interaction, especially if the mutual solute−solvent polarization is neglected. Further, in their discussion Levy et al. observe that the shift to the $n \rightarrow \pi^*$ absorption band computed with the same all-classical method is much larger than the shift they computed with a quantum chemical treatment. There are thus several reasons why our value would differ from this first published theoretical calculation of the solvent shift to the $\pi^* \rightarrow n$ transition in formaldehyde. With an integral equation treatment (called the reference interaction site model (RISM)) of the solvent and the HF quantum chemical method, Ten-no et al. compute a shift of 0.035 eV with the gas-phase optimal geometry for the first excited state of formaldehyde.[11] The model only accounts for pairwise interactions. Integral equations can account for specific interactions and are generally computationally more efficient than simulations but not as accurate; the HF method is not optimal for the description of excited states. Despite these differences, the estimate by Ten-no et al. is close to ours. The continuum calculations of Sánchez et al. for the relaxed nonplanar structure of excited formaldehyde give blue shifts of 0.082 and 0.033 eV with the singles-configuration interaction (CIS) method and the singles- and doubles-CI (CISD) method, respectively.[12] The nonequilibrium solvation of the final state is accounted for, and the CI method is suitable for calculations on excited states and also accounts for dynamic correlation. A continuum description of the solvent fails, on the other hand, to account for specific interaction such as hydrogen bonding, although for this molecule, as we argue above, this type of interaction will be more important in calculations on solvent shifts to the $n \rightarrow \pi^*$ absorption than on the reverse emission. The CISD estimate of Sánchez is also close to our estimate. From a set of cluster calculations with the semiempirical intermediate neglect of differential overlap (INDO) method with the CIS method to obtain the transition energy, Coutinho and Canuto obtain a solvent shift estimate of 0.20 eV.[13] The solvent configurations are obtained from a classical simulation with the parameters for the excited-state borrowed from the calculation by Levy et al. discussed above. The cluster calculation will guarantee that there is a correct intermolecular antisymmetry in contrast to our treatment that only give the intermolecular antisymmetry an approximate account. On the other hand, the merit of semiempirical methods

is moot, and even two recent reviews, that generally are sympathetic to semiempirical methods, point out that many such methods have problems to describe weak- and long-ranged electrostatic interactions as well as hydrogen bonding.[76,77] There is also the problem of the configuration sampling: unless the parameters used in the all-classical simulation are fairly accurate, the configurations will not be distributed correctly.

We can also compare the radial distribution functions in case there is an explicit solvent. The $H_2C-O\cdots O-H_2$ radial distribution of Levy et al. shows very little structure—not even a slight peak.[9] Although this limited knowledge of the solute−solvent distribution precludes certain conclusions, it seems that the solute−solvent interaction in the force field by Levy et al. is weaker than in our case where a peak in the discussed distribution is present. In contrast, the published $H_2C-O\cdots H-OH$ radial distribution of Coutinho and Canuto displays a clear peak, which indicates that hydrogen bonds have formed—a conclusion the authors also make.[13] The difference in solute−solvent interaction between our and the previous two studies—a difference the distributions confirm is there—explains in part why our solvent shifts differ. The greatest similarity with our results is found upon comparison with the results by Ten-no et al.[10,11] They have a clear peak for the oxygen atom in water, while the hydrogen atom in water shows no real peak; instead, it climbs with a relative small slope to its bulk value. This similarity with our result shows that it may be more than a cancellation that makes the estimate of the solvent shift of Ten-no et al. and the present estimate so similar, although a cancellation is far from ruled out given the differences between the models.

5. Summary

The present study computes the solvent shift to the fluorescence transition $\pi^* \rightarrow n$ in formaldehyde in water with an ab initio model with explicit solvent that includes a nonelectrostatic perturbation to the solute from the solvent. The model is able to satisfactorily reproduce a selection of supermolecular CASPT2 pair potentials for both ground and the relevant excited state, $S_1(n,\pi^*)$. Two different basis sets are used: their average solvent shift coincides while the distribution of the less contracted basis set shows a wider distribution which is argued to come from the larger polarizability of formaldehyde described in that basis set. Our computed shift is smaller than all other previous studies. Also, in contrast to our previous study of the $n \rightarrow \pi^*$ absorption, the packing strain of the final state (vertical deexcited ground state) has no effect on the average solvent shift, only on its distribution.

References and Notes

(1) Tomasi, J.; Persico, M. *Chem. Rev.* **1994**, *94*, 2027−2094.

(2) Luque, F. J.; Curutchet, C.; Muñoz-Muriedas, J.; Bidon-Chanal, A.; Soteras, I.; Morreale, A.; Gelp×c1, J. L.; Orozco, M. *Phys. Chem. Chem. Phys.* **2003**, *5*, 3827−3836.

(3) Ángyán, J. G.; Náray-Szabó, G. In *Theoretical Models of Chemical Bonding*; Maksiæ, Z. B., Ed.; Springer: Berlin, 1991; Vol. 4, pp 1−49.

(4) van Duuren, B. L. *Chem. Rev.* **1963**, *63*, 325−354.

(5) Jameson, D. M.; Croney, J. C.; Moens, P. D. J. *Methods Enzymol.* **2003**, *360*, 1−43.

(6) Tinnefeld, P.; Sauer, M. *Angew. Chem., Int. Ed.* **2005**, *44*, 2642−2671.

(7) Lakowicz, J. R. *Principles of Fluorescence Spectroscopy*, 2nd ed.; Kluwer Academic/Plenum: New York, 1999.

(8) Öhrn, A.; Karlström, G. *Mol. Phys.*, in press.

(9) Levy, R. M.; Kitchen, D. B.; Blair, J. T.; Krogh-Jespersen, K. *J. Phys. Chem.* **1990**, *94*, 4470−4476.

(10) Ten-no, S.; Hirata, F.; Kato, S. *Chem. Phys. Lett.* **1993**, *214*, 391−396.

(11) Ten-no, S.; Hirata, F.; Kato, S. *J. Chem. Phys.* **1994**, *100*, 7443−7453.

(12) Sánchez, M. L.; Aguilar, M. A.; Olivares del Valle, F. J. *J. Phys. Chem.* **1995**, *99*, 15758−15764.

(13) Coutinho, K.; Canuto, S. *J. Chem. Phys.* **2000**, *113*, 9132−9139.

(14) Friedman, H. L. *Mol. Phys.* **1975**, *29*, 1533−1543.

(15) Cui, Q. *J. Chem. Phys.* **2002**, *117*, 4720−4728.

(16) Crescenzi, O.; Pavone, M.; De Angelis, F.; Barone. V. *J. Phys. Chem. B* **2005**, *109*, 445−453.

(17) Metropolis, N. A.; Rosenbluth, W.; Rosenbluth, M. N.; Teller, A. H.; Teller, E. *J. Chem. Phys.* **1953**, *21*, 1087−1092.

(18) Moriarty, N. W.; Karlström, G. *J. Phys. Chem.* **1996**, *100*, 17791−17796.

(19) Wallqvist, A.; Ahlström, P.; Karlström, G. *J. Phys. Chem.* **1990**, *94*, 1649−1656.

(20) Roos, B. O.; Taylor, P. R.; Siegbahn, P. E. M. *Chem. Phys.* **1980**, *48*, 157−173.

(21) Roos, B. O. *Adv. Chem. Phys.* **1987**, *69*, 399−445.

(22) Roos, B. O.; Andersson, K.; Fülscher, M. P. *Chem. Phys. Lett.* **1992**, *192*, 5−13.

(23) Serrano-Andrés L.; Roos B. O. *Chem.—Eur. J.* **1997**, *3*, 717−725.

(24) Bauschlicher, C. W.; Langhoff, S. R. *Chem. Rev.* **1991**, *91*, 701−718.

(25) Malmqvist, P.-Å. *Int. J. Quantum Chem.* **1986**, *30*, 479−494.

(26) Malmqvist, P.-Å.; Roos, B. O. *Chem. Phys. Lett.* **1989**, *155*, 189−194.

(27) Malmqvist, P.-Å.; Roos, B. O.; Schimmelpfennig, B. *Chem. Phys. Lett.* **2002**, *357*, 230−240.

(28) Loeffler, H. H.; Rode, B. M. *J. Chem. Phys.* **2002**, *117*, 110−117.

(29) Nowak, R.; Bernstein, E. R. *J. Chem. Phys.* **1987**, *87*, 2457−2465.

(30) Zipp, A.; Kauzmann, W. *J. Chem. Phys.* **1973**, *59*, 4215−4224.

(31) Bayliss, N. S.; McRae, E. G. *J. Phys. Chem.* **1954**, *58*, 1002−1006.

(32) Reichardt, C. *Solvents and Solvent Effects in Organic Chemistry*, 3rd ed.; Wiley: Weinheim, 2003.

(33) Price, W. C.; Sherman, W. F.; Wilkinson, G. R. *Proc. R. Soc. London, Ser. A* **1960**, *255*, 5−21.

(34) Surján, P.; Ángyán, J. G. *Chem. Phys. Lett.* **1994**, *225*, 258−264.

(35) Chalmet, S.; Ruiz-López, M. F. *Chem. Phys. Lett.* **2000**, *329*, 154−159.

(36) Patkowski, K.; Jeziorski, B.; Szalewicz, K. *J. Chem. Phys.* **2004**, *120*, 6849−6862.

(37) Dobrosavljevč, V.; Henebry, C. W.; Stratt, R. M. *J. Chem. Phys.* **1988**, *88*, 5781−5789.

(38) Dobrosavljevič, V.; Henebry, C. W.; Stratt, R. M. *J. Chem. Phys.* **1989**, *91*, 2470−2478.

(39) Stratt, R. M.; Adams, J. E. *J. Chem. Phys.* **1993**, *99*, 775−788.

(40) Öhrn, A.; Karlström, G. *J. Phys. Chem. B* **2004**, *108*, 8452−8459.

(41) Moriarty, N. W.; Karlström, G. *J. Chem. Phys.* **1997**, *105*, 6470−6474.

(42) Hermida-Ramón, J. M.; Karlström, G. *J. Phys. Chem. A* **2003**, *107*, 5217−5222.

(43) Hermida-Ramón, J. M.; Karlström, G. *J. Mol. Struct. THEOCHEM* **2004**, *712*, 167−173.

(44) Szasz, L. *Pseudopotential Theory of Atoms and Molecules*; Wiley: New York, 1985.

(45) Barandiarán, Z.; Seijo, L. *J. Chem. Phys.* **1988**, *89*, 5739−5746.

(46) Abarenkov, I. V.; Antonova, I. M. *Int. J. Quantum Chem.* **2004**, *100*, 649−660.

(47) Yoshida, N.; Kato, S. *J. Chem. Phys.* **2000**, *113*, 4974−4984.

(48) Nagarajan, V.; Wesolowski, T. A.; Warshel, A. *J. Chem. Phys.* **1992**, *97*, 4264−4271.

(49) Valderrama, E.; Wheatley, R. J. *J. Comput. Chem.* **2003**, *24*, 2075−2082.

(50) Schnitker, J.; Rossky, P. J. *J. Chem. Phys.* **1987**, *86*, 3462−3470.

(51) Hart, E. J.; Boag, J. W. *J. Am. Chem. Soc.* **1962**, *84*, 4090−4095.

(52) Jeziorski, B.; Bulski, M.; Piela, L. *Int. J. Quantum Chem.* **1976**, *10*, 281−297.

(53) Bulski, M.; Chaasiñski, G.; Jeziorski, B. *Theor. Chim. Acta* **1979**, *52*, 93−101.

(54) Margenau, H.; Kestnar, N. R. *Theory of Intermolecular Forces*; Pergamon: Oxford, 1969.

(55) Pierloot, K.; Dumez, B.; Widmark, P.-O.; Roos, B. O. *Theor. Chim. Acta* **1995**, *90*, 87−114.

(56) Widmark, P.-O.; Malmqvist, P.-Å.; Roos, B. O. *Theor. Chim. Acta* **1990**, *77*, 291−306.

(57) Stålring, J.; Bernhardsson, A.; Lindh, R. *Mol. Phys.* **2001**, *99*, 103−114.

(58) Andersson, K.; Malmqvist, P.-Å.; Roos, B. O.; Sadlej, A. J.; Wolinski, K. *J. Phys. Chem.* **1990**, *94*, 5483−5488.

(59) Andersson, K.; Malmqvist, P.-Å.; Roos, B. O. *J. Chem. Phys.* **1992**, *96*, 1218−1226.

(60) Roos, B. O.; Andersson, K.; Fülscher, M. P.; Malmqvist, P.-Å.; Serrano-Andrés, L.; Pierloot, K.; Merchán, M. *Adv. Chem. Phys.* **1996**, *93*, 219−331.
(61) van Duijneveldt, F. B.; van Duijneveldt-van de Rijdt, J. G. C. M.; van Lenthe, J. H. *Chem. Rev.* **1994**, *94*, 1873−1885.
(62) Mayer, I. *Int. J. Quantum Chem.* **2004**, *100*, 559−566.
(63) Karlström, G.; Lindh, R.; Malmqvist, P.-Å.; Roos, B. O.; Ryde, U.; Veryazov, V.; Widmark, P.-O.; Cossi, M.; Schimmelpfennig, B.; Neogrady, P.; Seijo, L. *Comput. Mater. Sci.* **2003**, *28*, 222−239.
(64) Walsh, A. D. *J. Chem. Soc.* **1953**, 2306−2317.
(65) Brand, J. C. D. *J. Chem. Soc.* **1956**, 858−872.
(66) Merchán, M.; Roos, B. O. *Theor. Chim. Acta* **1995**, *92*, 227−239.
(67) Hachey, M. R. J.; Bruna, P. J.; Grein, F. *J. Mol. Spectrosc.* **1996**, *176*, 375−384.
(68) Angeli, C.; Borini, S.; Ferrighi, L.; Cimiraglia, R. *J. Mol. Struct. THEOCHEM* **2005**, *718*, 55−69.
(69) Laane, J. In *Structure and Dynamics of Electronic Excited States*; Laane, J., Takahashi, H., Bandrauk, A. D., Eds.; Springer: Berlin, 1999; pp 3−35.
(70) Zwanzig, R. W. *J. Chem. Phys.* **1954**, *22*, 1420−1426.
(71) Kofke, D. A. *Mol. Phys.* **2004**, *102*, 405−420.
(72) Böttcher, C. J. F. *The Theory of Electric Polarization*; Elsevier: Amsterdam, 1973; Vol. 1.
(73) Renkes, G. D.; Wettack, F. S. *J. Am. Chem. Soc.* **1969**, *91*, 7514−7515.
(74) O'Sullivan, M.; Testa, A. C. *J. Am. Chem. Soc.* **1970**, *92*, 5842−5844.
(75) Röhrig, U. F.; Frank, I.; Hutter, J.; Alessandro, L.; VandeVondele, J.; Rothlisberger, U. *ChemPhysChem* **2003**, *4*, 1177−1182.
(76) Winget, P.; Selçuki, C.; Horn, A. H. C.; Martin, B.; Clark, T. *Theor. Chem. Acc.* **2003**, *110*, 254−266.
(77) Bredow, T.; Jug, K. *Theor. Chem. Acc.* **2005**, *113*, 1−14.